

Cyclic Voltammetry and Molecular Docking Study of the Interactions of Two Derivatives of 5-fluorouracil with DNA

Da-An Qin, Xiao-Qing Cai, Qian Miao, Zuo-Hui Wang, Mao-Lin Hu*

College of Chemistry and Materials Engineering, Wenzhou University, Wenzhou 325035, China

*E-mail: maolin@wzu.edu.cn

Received: 6 November 2013 / Accepted: 28 December 2013 / Published: 2 February 2014

Two derivatives of 5-fluorouracil (5-FU) with similar structure were synthesised, and their interactions with calf thymus-DNA (CT-DNA) have been studied using cyclic voltammetry (CV) at a DNA-modified gold electrode. The variations in the cyclic voltammetric behaviour of different concentrations of drugs with CT-DNA have been investigated. Molecular docking was used to predict the modes of interactions of the drugs with DNA. The molecular docking results indicated that the modes of interactions between two drugs and DNA helix can be considered as groove binding. To measure the binding ability of the two drugs with DNA, binding constants (K) were calculated from voltammetric data, i.e., and the binding free energies of the two drugs with DNA were calculated using the AMBER software package. For the binding strength, the computational results complemented the experimental results.

Keywords: Cyclic voltammetry; 5- Fluorouracil derivatives; Binding constants; Molecular docking; Binding free energies

1. INTRODUCTION

The interactions of DNA with several drug molecules play a key role in the life sciences and drug design and have attracted considerable attention [1] because of analytic results that provide insight into the mechanism of action of DNA-targeted drugs. The dominant binding modes of small molecules with DNA can be categorised into two major classes: (i) covalent binding and (ii) non-covalent binding, including intercalative binding [2], nonspecific electrostatic interaction [3] and DNA major/minor groove binding [2]. Non-covalent binding is the predominant DNA-binding mode of the two classes of small ligands [4–7]. Numerous techniques have been developed to investigate these interactions, including NMR [8], UV–vis spectroscopy [9], fluorescence [10] and phosphorescence [11]. However, a majority of these techniques have limitations. Currently, electrochemical methods,

especially cyclic voltammetry, appear to be much more elegant for use in exploring these interactions due to faster analysis using low cost, simpler and smaller devices with respect to the other methods [12].

In recent years, there has been a growing interest in the CV investigations of the interactions between anticancer drugs and DNA. Shah [13] reported the interaction of hydantoin derivatives with CT-DNA using CV, and Temerk et al. [14,15] studied the interaction of the antitumor drugs with dsDNA via CV. Observing the pre- and post-electrochemical signals of DNA provides good evidence for determining the interaction mechanism. An electrochemical approach can provide new insight into rational drug design and would lead to increased understanding of the interaction mechanism between anticancer drugs and DNA .

Molecular docking techniques play an important role in drug design and were applied to describe the most probable mode of DNA binding. When used prior to experimental screening, DOCK [16-18], AutoDock and molecular operating environment (MOE) can be considered powerful computational filters and enable a reduction in the cost and labour required for the development of potent medicinal drugs. Docking techniques will undoubtedly continue to play an important role in drug discovery.

5-FU is a fluoropyrimidine-type compound with marked anti-tumour effects [19] and is widely used in the treatment of solid malignant tumours, particularly colorectal carcinoma. Its biological or chemical triggering mechanism of action is well understood [20-22]. Because of its toxic side effects, several prodrug systems, such as amines, alcohols, and peptides [23], are exploited to improve its anticancer activity and minimise the toxic side effects.

Although 5-FU and DNA interact via intercalation [24], the modes of interactions of its derivatives with DNA are still unknown. In our work, two types of structurally similar amides of 5-FU were synthesised. CV was carried out to determine the interactions of the two drugs with CT-DNA. The changes in the cyclic voltammograms upon the addition of various concentrations of drugs help to probe the strength of interactions between the two drugs and CT-DNA. A detailed comparison and investigation of the docking behaviour of the two anticancer drugs with DNA has been carried out using experimental and theoretical methods. Furthermore, the structure-activity relationship has been explained by calculating the binding free energies using the AMBER software package version ff03 [25].

2. EXPERIMENTAL

2.1. Apparatus and reagents

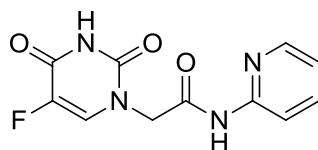
Tris-HCl was obtained commercially. Calf thymus DNA with high molecular weight was extracted and purified by a method described elsewhere [26]. Other chemicals were of analytical reagent grade and used as received. Supporting electrolyte for all experiments was a 0.1 M KCl / 0.05 M Tris-HCl buffer solution and the 0.05 M Tris-HCl buffer solution was adjusted to pH 7.16 by HCl. The DNA solution was prepared with 0.1 M KCl / 0.05 M Tris-HCl (pH 7.16) and stored at 4 °C. The

concentration of DNA (nucleotide phosphate) was determined by UV absorbance at 260 nm. The extinction coefficient, ϵ_{260} , was taken as $6600 \text{ M}^{-1} \text{ cm}^{-1}$ [27].

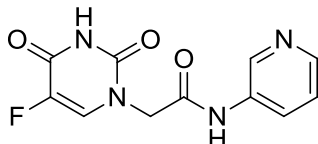
All the electrochemical measurements were performed on a CHI1030b electrochemical workstation (CH Instrumental, Chenhua Corp., Shanghai, China). ^1H NMR and ^{13}C NMR spectra were recorded on a AVANCE-500 instrument using tetramethylsilane (TMS) as an internal standard and $\text{DMSO-}d_6$ as the solvent at room temperature. Chemical shifts are given in relative to TMS, coupling constants (J) are expressed in Hz. IR spectra were taken on an EQUINOX-55 instrument.

2.2. Synthesis of the compounds O and M

The two derivatives of 5-FU were synthesised in our laboratory according to a previously published method [28]. These drugs shared a similar structure that only differed in the location of the functional group, which was located at the ortho position of one compound (Scheme 1, O) and the meta position of the other compound (Scheme 1, M).



2-(5-fluoro-2,4-dioxo-3,4-dihydropyrimidin-1(2H)-yl)-N-(pyridin-2-yl)acetamide (O)



2-(5-fluoro-2,4-dioxo-3,4-dihydropyrimidin-1(2H)-yl)-N-(pyridin-3-yl)acetamide (M)

Scheme 1. Molecular structures of Ortho compound (O) and Meta compound (M).

The compound O was prepared in 2 steps. First, 5-fluorouracil-1-acetic acid (5-FUA) was prepared using a previously described general method [29]. Second, The compound O was synthesised from 5-FUA, dicyclohexyl carbodiimide (DCC), 1-hydroxybenzotriazole (HOBt) as follows: A solution of DCC (1.52 g, 5.6 mmol) in DMF (10 mL) was dropped in a DMF solution (20 mL) of 5-FUA (1.05 g, 5.6 mmol) and HOBt (0.85g , 5.6 mmol) at 0°C over a period of 40 min. The resulting solution was stirred at room temperature over the night. Appropriate pyridin-2-amine (5.6 mmol) was added to the above mixture. After stirring 4 hours, a white solid was obtained. After filtration, the filtrate was concentrated under vacuum. The residue was separated by column chromatography to yield compound O. ^1H NMR (500 MHz, DMSO, ppm) δ 11.92 (1H, s , NH), 8.08 (1H, d, $J = 6.8$ Hz, FCCH), 7.88 (1H, dd, $J = 5.1$ Hz, C6H, Py), 7.45–7.34 (1H, m, C2H, Py), 6.49 (1H, dd, $J = 5.0, 3.5$ Hz, C4H, Py), 6.47 (1H, d, $J = 4.7$ Hz, C5H, Py), 6.17(1H, s, NHCOCH₂), 4.33 (2H, s, CH₂). ^{13}C NMR (126 MHz, DMSO) δ 169.59 (NHCO), 159.20 (d, $J_{\text{C-F}} = 2.6$ Hz, C4, 5-Fu), 157.47 (d, $J_{\text{C-F}} =$

25.7 Hz, C2, 5-Fu), 149.66 (C2, Py), 146.34 (C6, Py), 139.26 (d, $J_{C-F} = 228.6$ Hz, C5, 5-Fu), 137.67 (C4, Py), 130.65 (d, $J_{C-F} = 33.8$ Hz, C6, 5-Fu), 111.75 (C5, Py), 108.54 (C3, Py), 48.85 (CH₂). IR (KBr, cm⁻¹): 3063 (N–H stretching vibration), 2830 (= C–H stretching vibration), 1702 (C=O stretching vibration), 1584 (C=C and C=N stretching vibration), 1487 (N–H deformation and C–N stretching vibration), 1427 (C–H blending vibration), 1306 (Mixed C–N stretching and N–H bending vibrations), 749 (C–H deformation vibration of pyridine ring), 730 (pyridine ring deformation vibration).

The synthetic process of M was the same as described for O. Appropriate pyridin-3-amine (5.6 mmol) was used instead of pyridin-3-amine. ¹H NMR (500 MHz, DMSO) δ 11.93 (1H, d, $J = 5.1$ Hz, 1H), 10.51 (1H, s, NHCOCH₂), 8.72 (d, $J = 1.2$ Hz, C2H, Py), 8.29 (1H, d, $J = 4.0$ Hz, C6H, Py), 8.09 (1H, dd, $J = 11.9, 6.8$ Hz, FCCH), 8.03 – 7.97 (1H, m, C4H, Py), 7.37 (1H, dd, $J = 8.3, 4.7$ Hz, C5H, Py), 4.36 (2H, s, CH₂). ¹³C NMR (126 MHz, DMSO) δ 169.26 (NHCO), 166.00 (C6, Py), 157.52 (d, $J_{C-F} = 25.8$ Hz, C4, 5-Fu), 149.72 (d, $J_{C-F} = 18.0$ Hz, C2, 5-Fu), 144.61 (C2, Py), 140.45 (d, $J_{C-F} = 63.3$ Hz, C5, 5-Fu), 138.38 (C3, Py), 130.77 (dd, $J_{C-F} = 63.7, 33.9$ Hz, C6, 5-Fu), 126.17 (C4, Py), 123.79 (C5, Py), 50.16 (CH₂). IR (KBr, cm⁻¹): 3304 (N–H stretching vibration), 3075 (=C–H stretching vibration), 1664 (C=O stretching vibration), 1590 (C=C and C=N stretching vibration), 1558 (N–H deformation and C–N stretching vibration), 1427 (C–H blending vibration), 1281 (Mixed C–N stretching and N–H bending vibrations), 804 (C–H deformation vibration of pyridine ring), 706 (pyridine ring deformation vibration).

2.3. Preparation of DNA-modified electrode

The electrodes that were modified with DNA were prepared according to the previous studies [30, 31]. Gold disk electrodes were polished with a series of alumina powder (1.0, 0.5 and 0.05 μm). Then, the Au electrode was purified and placed in fresh piranha solution (30% H₂O₂ and 70% H₂SO₄) to remove adsorbed organic impurities and sonicated in highly purified water for 5 min. Prior to the modification, the electrode surface was electrochemically activated by sweeping from -0.3 to +1.5 V in 0.1 M H₂SO₄ until a stable cyclic voltammogram characteristic of a clean Au electrode was obtained. After washing with double-distilled water, the freshly polished Au electrode was immediately modified by transferring a droplet of 10 μL of 1.0 μg μL⁻¹ CT-DNA solution onto its surface, followed by air-drying overnight. The DNA-modified electrode (denoted as CT-DNA/ Au throughout) was then soaked in sterile water for about 4 h and again rinsed with water to remove any unadsorbed CT-DNA.

2.4. Cyclic voltammetry

Voltammetric measurements were carried out in a conventional three-electrode cell consisting of a bare gold or CT-DNA/ Au as the working electrode, a saturated calomel electrode (SCE), and a platinum wire auxiliary electrode. We used typical CV experiments utilised a 5 mM solution of K₃[Fe(CN)₆] / K₄[Fe(CN)₆] (1:1) in 0.05 M Tris–HCl buffer at pH 7.16 with 0.1 M KCl at room temperature (25 °C). All solutions were deaerated with highly pure nitrogen, and the electrochemical experiments were performed with a CHI 1030b electrochemical workstation (Shanghai Chenhua Co.) at a scan rate of 0.1 V s⁻¹.

2.5. Molecular docking

Docking operations were performed using version 4.0 of the AutoDock program package and the Lamarckian genetic algorithm (LGA) available in AutoDock 4.0, which was proven to be most reliable, successful and effective [17, 32]. The LGA was used in this docking study of compounds O and M with double-stranded DNA. The DNA duplex receptor structure from the Protein Data Bank (PDB ID 2dyw) contained 12 base pairs. The base pair sequence was CGCGAATTCGCG : GCGCTTAAGCGC. All water molecules and ligands that co-crystallised with the DNA were removed from the original structure. Then, the compounds and DNA were added along with Gasteiger charges and polar hydrogen atoms using AutoDockTools (ADT) version 1.5.2. AutoGrid was used to calculate the grid maps that represented the DNA in the docking process. Sufficiently large grids were chosen to include a significant part of the DNA. In all cases, we used grid maps with a grid box size of $106 \times 110 \times 102$ points with a grid-point spacing of 0.375 \AA . Then, we began to conduct the molecular docking via the LGA using default parameters. For each ligand, fifty independent docking runs were carried out.

3. RESULTS AND DISCUSSION

3.1. Electrochemical characterization of CT-DNA/ Au

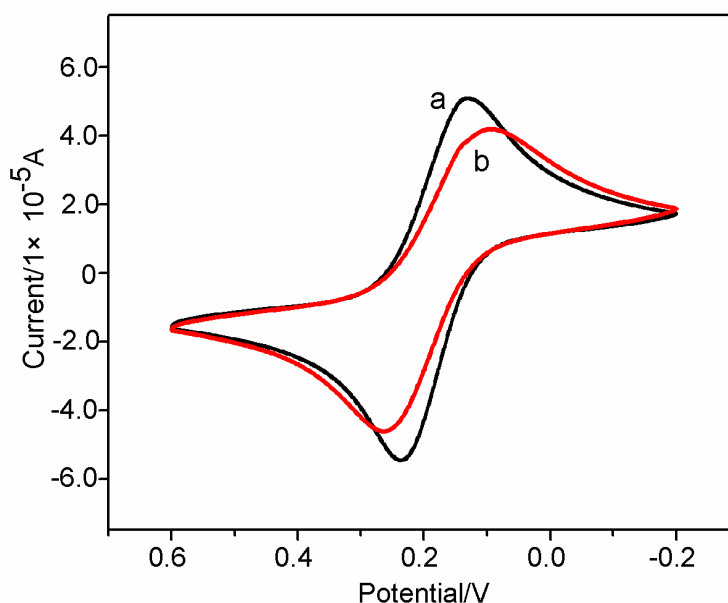


Figure 1. Cyclic voltammograms of $\text{Fe}(\text{CN})_6^{3-/4-}$ in pH 7.16 Tris–HCl buffer solution at a bare Au electrode (a), CT-DNA/ Au (b). The scan rate is 0.1 V s^{-1} and the concentrations of $\text{Fe}(\text{CN})_6^{3-/4-}$ and KCl are 5 mM.

Figure 1 represents the typical cyclic voltammograms of the bare Au electrode (curve a) and CT-DNA/ Au (curve b) in 5.0 mM $\text{Fe}(\text{CN})_6^{3- / 4-}$ solution at a scanning rate of 0.1 V s^{-1} , where two well-defined redox peaks were achieved in both cases. Moreover, there was an obvious decrease in the peak current at CT-DNA/ Au compared with bare Au electrode. This can be attributed to DNA acted as an electron and mass transfer blocking layer, which hindered the diffusion of $\text{Fe}(\text{CN})_6^{3- / 4-}$ toward the electrode surface. The result also confirms that DNA is well modified on the surface of Au electrode. CV of the DNA-modified Au electrode remained stable after 20 scans in the Tris-HCl buffer solution, demonstrating the electrochemical stability of the DNA films.

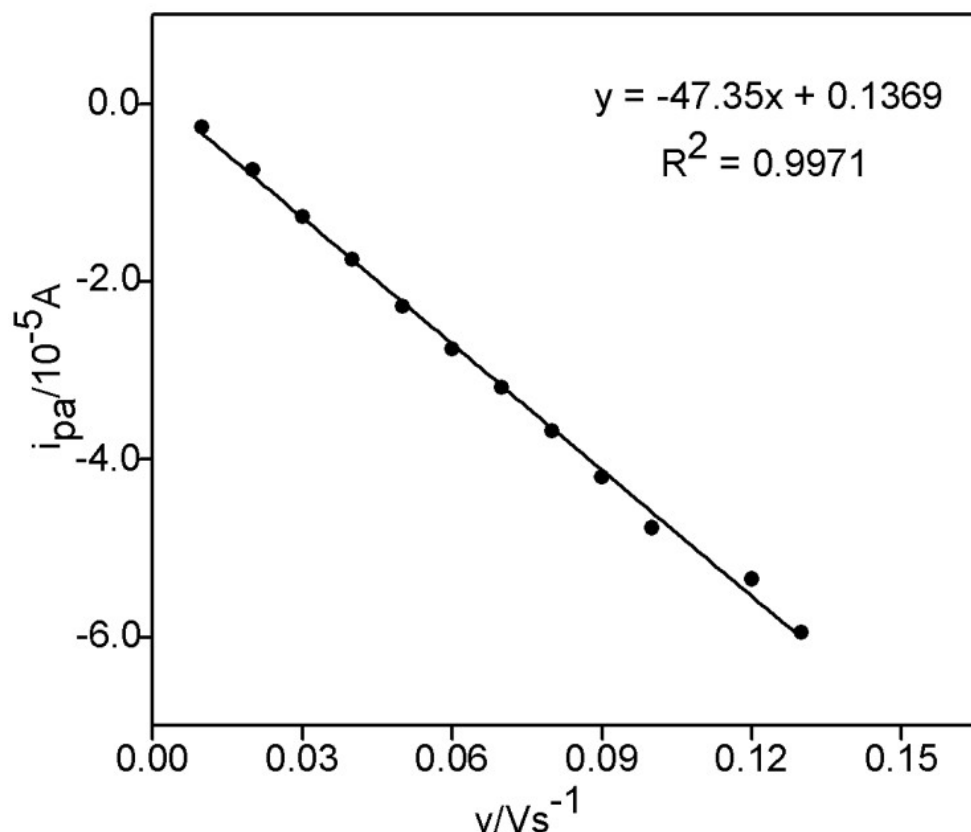


Figure 2. The relationship between anodic peak current and the scanning rate ($0.01\sim 0.13 \text{ V s}^{-1}$) for CT-DNA/ Au.

The electrochemical behaviors of $\text{Fe}(\text{CN})_6^{3- / 4-}$ at CT-DNA/ Au were further studied with a change in scan rate in Tris-HCl buffer solution (pH 7.14) containing 5 mM $\text{Fe}(\text{CN})_6^{3- / 4-}$. As shown in Fig.2, it can be clearly found that the anodic peak currents increased upon the increase of the scan rate, and a good linearity between peak current and scan rate could be obtained within the range of $0.01\sim 0.13 \text{ V s}^{-1}$. These results reveal that the electrochemical kinetics is a typical surface adsorption-controlled electrochemical process [33, 34].

3.2. Interaction of drugs with the DNA-modified Au electrode

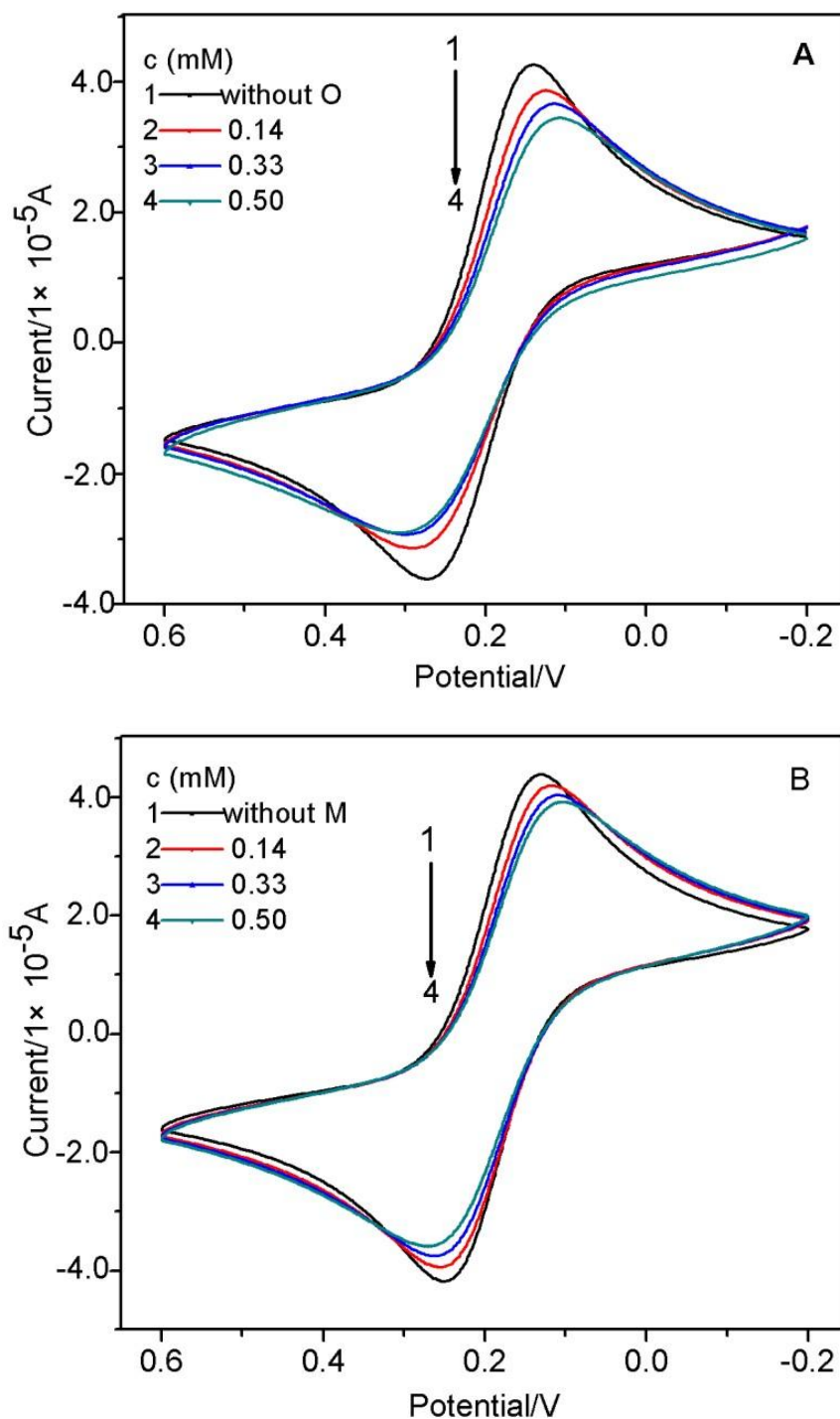


Figure 3. Cyclic voltammograms of $\text{Fe}(\text{CN})_6^{3-/4-}$ in Tris-HCl buffer solution (pH 7.16) containing different concentrations of drugs: (A) O; (B) M. The scan rate is 0.1 V s^{-1} and the concentrations of $\text{Fe}(\text{CN})_6^{3-/4-}$ and KCl are 5 mM.

Compounds O and M are non-electroactive organic small molecules. $\text{Fe}(\text{CN})_6^{3-/4-}$ was used as an redox probe [35] to investigate the interactions of non-electroactive of small molecules with CT-

DNA. Cyclic voltammograms changes of $\text{Fe}(\text{CN})_6^{3- / 4-}$ on different concentrations of O or M at CT-DNA/ Au were shown in (Fig.3). As is evidence from Fig.3A, both the reduction and oxidation peak currents gradually decrease accompanied an increase in the seven different concentrations from 0.077 mM to 0.50 mM of O (some concentrations were omitted in Figures). Similar phenomena were obtained for M (Fig.3B). The maximum oxidation peak current changes were 1.21×10^{-5} A, 1.023×10^{-5} A, respectively. The reason can be attributed that DNA films makes the redox process of $\text{Fe}(\text{CN})_6^{3- / 4-}$ marker at the Au electrode more difficult due to the physical blockage as well as possible electrostatic repulsion. When the prodrugs were added to the solution, they interacted with DNAs to cause the DNA film denser, making the migration of $\text{Fe}(\text{CN})_6^{3- / 4-}$ ions through the film harder. As a result, the redox peak current of $\text{Fe}(\text{CN})_6^{3- / 4-}$ decreased.

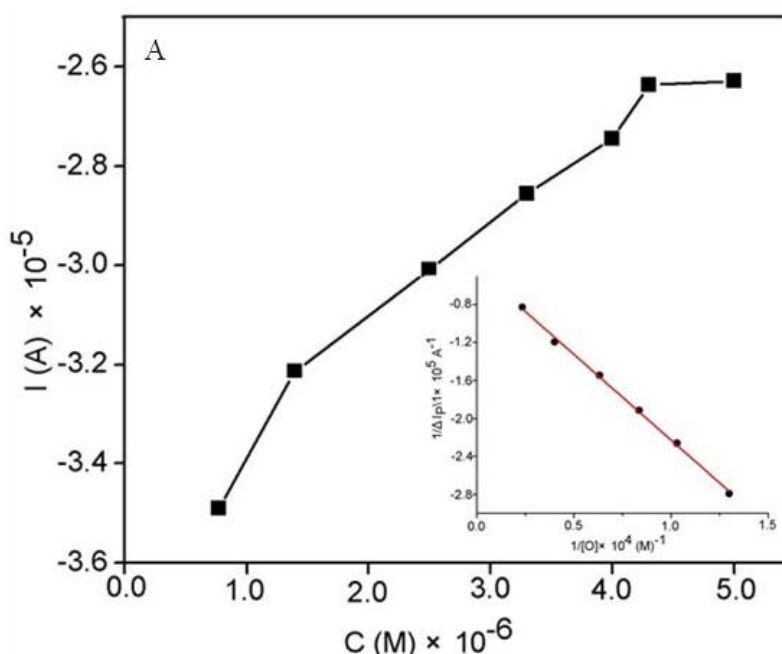
Table 1. The binding constants (K) and the binding free energies (E) between the drugs and DNA.

Compound	$K \times 10^3 / (\text{L} \cdot \text{mol}^{-1})$	$E \times 10^3 / (\text{J} \cdot \text{mol}^{-1})$
O	2.33 ^a	-24.41
M	1.45 ^a	-22.43
5-FU	6.60 ^b	-

^aDetermined from the cyclic voltammetry data using a previously published equation [36].

^bFrom a previously published paper [38].

As can be seen from Fig. 4, both the peak currents of the cyclic voltammograms decreased with increasing the concentrations of drugs and tended to achieve a saturation value, as expected for Langmuir adsorption behaviour.



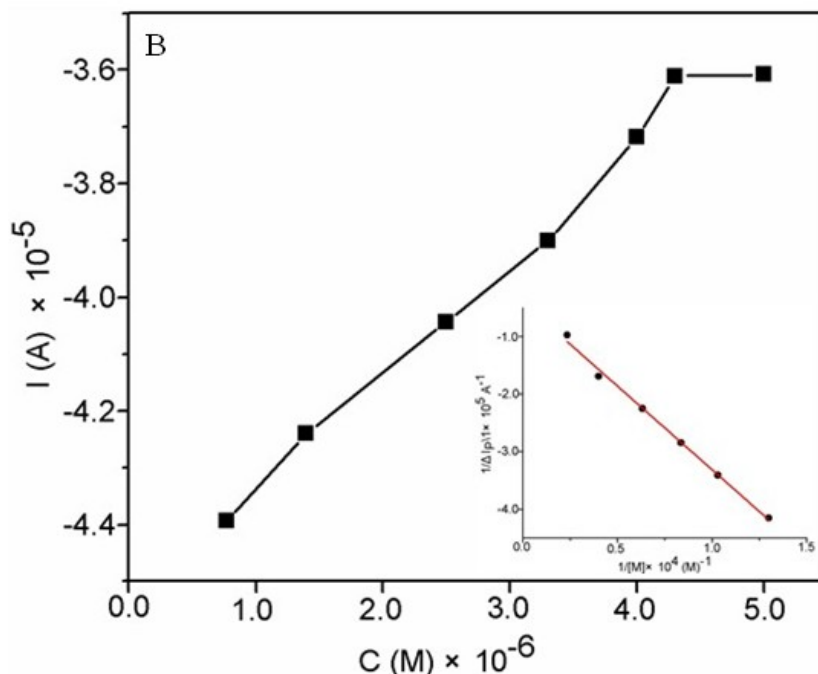


Figure 4. Adsorption isotherm of drugs: (A) O; (B) M on CT-DNA/ Au. The solid line is a fit to the Langmuir model. Inset: The relationship between $\frac{1}{[\text{DRUG}]}$ and $\frac{1}{\Delta I_p}$.

For a quantitative comparison of the binding strength of O and M with CT-DNA, the binding constant (K) between the test compounds and the CT-DNA was calculated (shown in Table 1) according to the Langmuir formula in Eq. (A.1) [35, 36]. According to the method of Qu et al. [37], it is assumed that DNA and DRUG only produce a single complex $\text{DNA} \cdot \text{DRUG}_m$.



The condition of binding constant is as follows:

$$K = \frac{[\text{DNA} \cdot \text{DRUG}_m]}{[\text{DNA}] \cdot [\text{DRUG}]^m} \quad (1.1)$$

And the following equations can be deduced

$$\Delta I_{\text{MAX}} = k' \cdot C_{\text{DNA}} \quad (1.2)$$

and

$$\Delta I = k' \cdot [\text{DNA} \cdot \text{DRUG}_m] \quad (1.3)$$

$$[\text{DNA}] + [\text{DNA} \cdot \text{DRUG}_m] = C_{\text{DNA}} \quad (1.4)$$

$$\Delta I_{\text{MAX}} - \Delta I = k' (C_{\text{DNA}} - [\text{DNA} \cdot \text{DRUG}_m]) \quad (1.5)$$

$$\Delta I_{\text{MAX}} - \Delta I = k' \cdot [\text{DNA}] \quad (1.6)$$

Put Eqs. (1.3) and (1.6) into (1.1) yields:

$$\log \frac{\Delta I}{\Delta I_{\text{MAX}} - \Delta I} = \log K + m \log [\text{DRUG}] \quad (1.7)$$

$$\frac{1}{\Delta I} = \frac{1}{\Delta I_{\text{MAX}}} + \frac{1}{\Delta I_{\text{MAX}} \cdot K} \cdot \frac{1}{[\text{DRUG}]^m} \quad (1.8)$$

To Eq. (1.8), we assumed $m = 1$, using ΔI_p represents ΔI , $\Delta I_{p,max}$ represents ΔI_{MAX} . As shown in Fig. 4 (inserted Pictures), $\frac{1}{[DRUG]}$ showed a good linear relationship with $\frac{1}{\Delta I_p}$, so the assumptive

value of m was reasonable. Thus, we got Eq. (A.1)

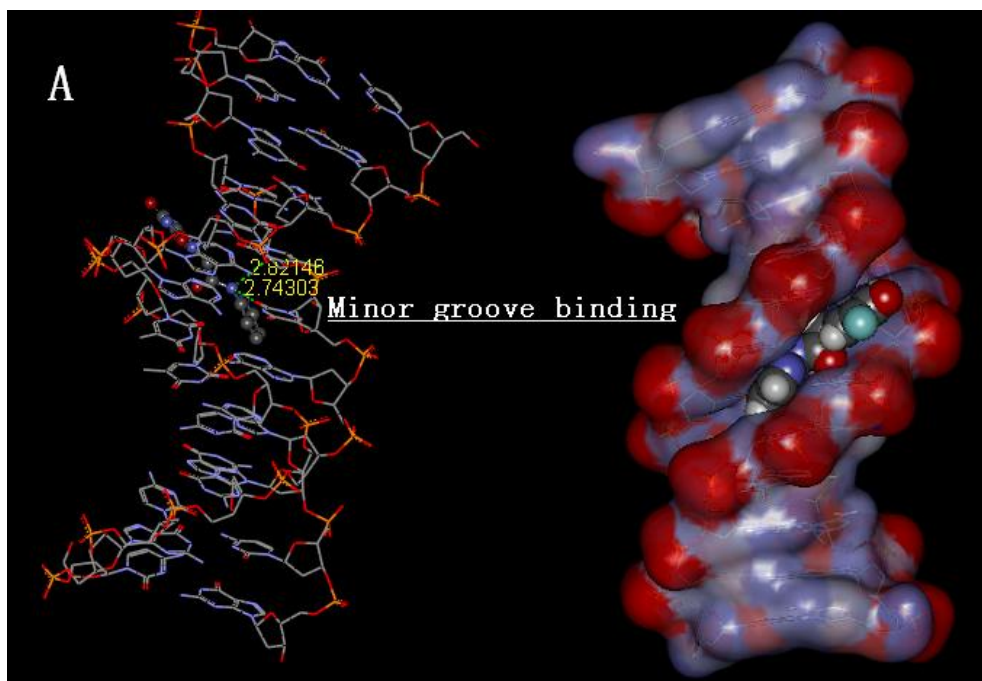
$$\frac{1}{\Delta I_p} = \frac{1}{\Delta I_{p,max}} + \frac{1}{\Delta I_{p,max} \cdot K} \cdot \frac{1}{[DRUG]} \quad \text{Eq. (A.1)}$$

where $\Delta I_p = I_{p0} - I_p$, I_p and I_{p0} represent the oxidation peak current of $\text{Fe}(\text{CN})_6^{3- /4-}$ in the presence and absence of the drugs, respectively; $\Delta I_{p,max}$ is the maximum difference of the oxidation peak current; and $[drug]$ represents the concentration of the drug. As a result, the binding constant (K) are $2.33 \times 10^3 \text{ L} \cdot \text{mol}^{-1}$ and $1.45 \times 10^3 \text{ L} \cdot \text{mol}^{-1}$ for O and M, respectively.

The binding constant of O is approximately 1.60 times larger than that of M, which may indicate that the CT-DNA-binding strength of O is stronger than that of M. The significant difference in the binding constants is chiefly because of the small structural difference between O and M in the position of the functional group. For 5-FU derivatives, stronger bonding to DNA indicates a more stable combination with DNA and thus better anticancer activity. These binding constants are much smaller than that of 5-FU, which means decreased toxic side effect [38]. Thus, we can conclude that O may be a more promising drug with higher anticancer activity than M. As a result, we can incorporate this new information into the design of a promising antitumor prodrug of 5-FU.

3.3. Molecular docking

In an effort to interpret the molecular mechanism for the interactions of O and M with DNA, molecular docking was performed to simulate the modes of interactions between the drugs and DNA [39-41].



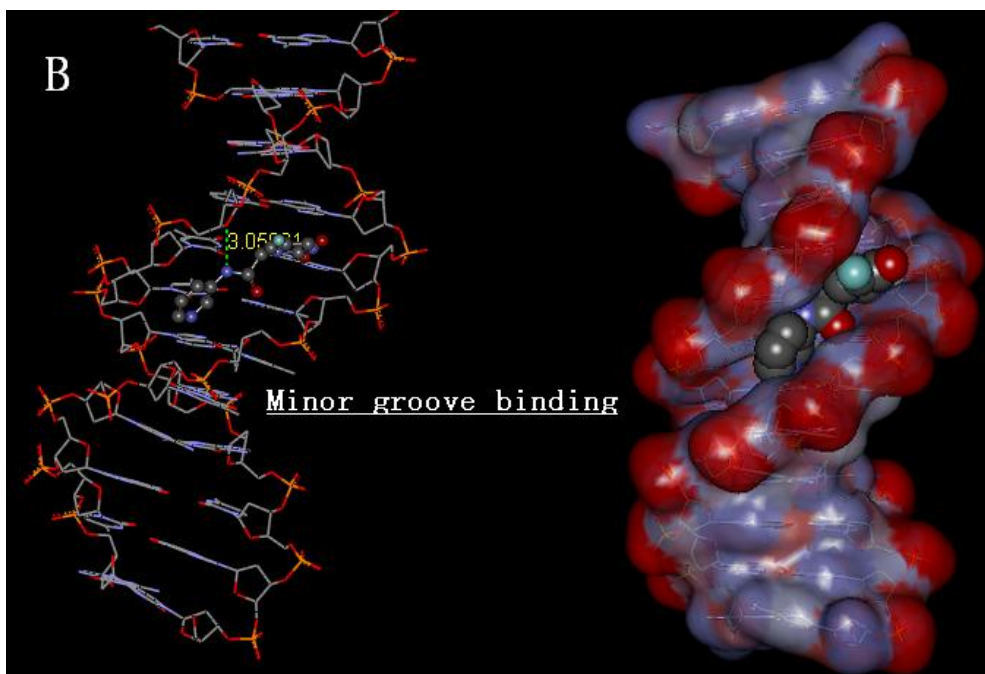


Figure 5. Binding of O (A) and M (B) into DNA

Minor groove binding makes intimate contacts with the walls of the groove, and as a result of this interaction, numerous hydrogen bonding and electrostatic interactions occur between a drug and DNA bases and its phosphate backbone [42]. As shown in Fig.5, in our work, there are two hydrogen bonds formed between compound O and DNA (Fig.5A). One is formed between compound O and number seven thymidine of one strand of DNA, with N atom serving as a hydrogen bond receptor (O(2)—H...N: 2.8246 Å), the other is formed between compound O and number eight thymidine of the same strand of DNA (O(4)—H...N: 2.70303 Å). As shown in Fig.5B, there is just a weak hydrogen bond formed between compound M and number nine cytosine of one strand of DNA, with N atom serving as a hydrogen bond receptor (O(4)—H...N: 3.05981 Å). The result indicates that the O binding with DNA is much more stable than M. It also shows that compounds O and M fit snugly into the curved contour of the targeted DNA in the minor groove, with the walls of the groove in close contact with pyrimidine and amide groups. As a result, we can draw a conclusion that the mode of interactions between two drugs and DNA helix can be considered as minor groove binding. In order to quantify the binding ability of the two drugs with DNA, the binding free energies between them and DNA were calculated according to the literature [25]. As shown in Table 1, the binding free energy of O and M are $-24.41 \times 10^3 \text{ J} \cdot \text{mol}^{-1}$ and $-22.43 \times 10^3 \text{ J} \cdot \text{mol}^{-1}$, respectively. The binding free energy of O is lower than that of M. Lower binding free energy indicates a more stable combination with DNA. Thus, we can conclude that the binding ability of O with DNA is stronger than that of M.

4. CONCLUSIONS

In this paper, two derivatives of 5-FU were synthesised, and their electrochemical behaviour

with CT-DNA were studied using cyclic voltammetry. Molecular docking was performed to simulate the modes of interactions between the drugs and DNA. The results demonstrate that their binding to DNA acts like groove binder which binds to the minor groove of DNA double helix. From the binding constants and the binding free energies, it can be concluded that the binding strength of the ortho compound is stronger than that of the meta compound. Therefore, we can make a bold guess that the ortho compound is a potential anticancer drug, which should be used in optimising the design of this class of 5-FU antitumor drugs.

ACKNOWLEDGEMENTS

This research is supported by the Natural Science Foundation of China (Nos. 21071111 and 21371137) and Commonweal Project of Science and Technology Department of Zhejiang Province (No. 2012C37010). We thank professor Shun Wang and Ji-Chang wang for many helpful discussions.

References

1. Z.S. Yang, D.P. Zhang, H.Y. Long, Y.C. Liu, *Electroanal. Chem.* 624 (2008) 91.
2. K.E. Erkkila, D.T. Odom, J.K. Barton, *Chem. Rev.* 99 (1999) 2777.
3. M.T. Carter, M. Rodriguez, A.J. Bard, *J. Am. Chem. Soc.* 111 (1989) 8901.
4. G. Bischoff, S. Hoffmann, *Curr. Med. Chem.* 9 (2002) 312.
5. X. Han, X. Gao, *Curr. Med. Chem.* 8 (2001) 551.
6. S. Neidle, C.M. Nunn, *Nat. Prod. Rep.* 15 (1998) 1.
7. R. Rohs, I. Bloch, H. Sklenar, Z. Shakked, *Nucleic Acids Res.* 33 (2005) 7048.
8. G. Zhang, D. Gao, J. Chao, S. Shuang, C. Dong, *Dyes Pigments* 82 (2009) 40.
9. J. Pastor, J.G. Siro, J.L. Garcia-Navio, J.J. Vaquero, J. Alvarez-Builla, F. Gago, B.de Pascual-Teresa, M. Pastpr, M.M. Rodrigo, *J. Org. Chem.* 62 (1997) 5476.
10. Y. Cao, X.W. He, *Spectrochim. Acta A* 54 (1998) 883.
11. J.F. Li, S.M. Shuang, C. Dong, *Talanta* 77 (2009) 1043.
12. H. Heli, S.Z. Bathaie, M.F. Mousavi, *Electrochim. Acta.* 51 (2005) 1108.
13. A. Shah, E. Nosheen, S. Munir, A. Badshah, R. Qureshi, Z. Rehman, Muhammad, H. Hussain, *J. Photochem. Photobiol., B.* 120 (2013) 90.
14. Y. M. Temerk, M. S. Ibrahim, M. Kotb, W. Schuhmann, *Anal. Bioanal. Chem.* 405 (2013) 3839.
15. A.E. Radi, H.M. Nassef, A. Eissa, *Electrochim. Acta.* 113 (2013) 164.
16. L.D. Wang, K. Zheng, Y.T. Li, Z.Y. Wu, C.W. Yan, *J. Mol. Struct.* 1037 (2013) 15.
17. A. Mandal, S. Ghosh, A. K. Bothra, A. Kumar N., P. Ghosh, *Euro. J. Med. Chem.* 54 (2012) 137
18. F. Arjmand, S. Parveen, M. Afzal, M. Shahid, *J. Photochem. Photobiol., B.* 114 (2012) 15.
19. C. Heidelberger, N.K. Chaudhuri, P. Danneberg, D. Mooren, L. Griesbach, R. Duschinsky, R.J. Schnitzer, E. Plevin, J. Scheiner, *Nature* 179 (1957) 663.
20. U.P. Singh, S. Kashyap, H.J. Singh, B.K. Mishra, P. Roy, A. Chakraborty, *J. Mol. Struct.* 01 (2012) 035.
21. J.B. Parker, J.T. Stivers, *Biochemistry* 50 (2011) 612.
22. Y. Fujinaka, K. Matsuokac, M. Imoria, M. Tuul, R. Sakasaid, *DNA Repair* 11 (2012) 247.
23. A. Conejo-Garcia, C.J. Schofield, *Bioorg. Med. Chem. Lett.* 15 (2005) 4004.
24. C.W. Ge, N.P. Wang, N. Gu, *Acta Chim. Sinica* 64 (2006) 1837.
25. N.N. Wei, A. Hamza, C. Hao, Z. Xiu, C.G. Zhan, *Theor Chem Acc.* 132 (2013) 1379.
26. S.Z. Bathaie, A.A. Moosavi-Movahedi, A.A. Saboury, *Nucleic Acid Res.* 27 (1999) 1001.
27. M.E. Reichmann, S.A. Rice, C.A. Thomas, P. Doty, *J. Am. Chem. Soc.* 76 (1954) 3047.
28. P. Yin, M.L. Hu, L.C. Hu, *J. Mol. Struct.* 882 (2008) 75.

29. C. Ausin, J.A. Ortega, J. Robles, A. Grandas, E. Pedroso, *Org. Lett.* 4 (2002) 4073.
30. D.W. Pang, H.D. Abruna, *Anal. Chem.* 70 (1998) 3162.
31. B.K. Jin, X.P. Ji, T. Nakamura, *Electrochim. Acta* 50 (2004) 1049.
32. L. Marinelli, A. Lavecchia, K.E. Gottschalk, E. Novellino, H. Kessler, *J. Med. Chem.* 46 (2003) 4393.
33. A.J. Bard, L.R. Faulkner, *Electrochemical Methods: Fundamentals and Applications*, 2nd ed., John Wiley, New York, 2001.
34. H.X. Ju, Y.K. Ye, Y.L. Zhu, *Electrochim. Acta.* 50 (2005) 1361.
35. K.J. Zhang, W.Y. Liu, *Int. J. Electrochem. Sci.* 6 (2011)1669.
36. S.Q. Liu, J. J. Xu, H. Y. Chen. *Colloids Surf. B: Biointerf.* 36 (2004)155.
37. F. Qu, N.Q. Li, Y.Y. Jiang, *Talanta.* 45 (1998) 787.
38. X.C. Li, K.G. Liu, D.A. Qin, C.C. Cheng, B.X. Chen, M.L. Hu, *J. Mol. Struct.* 1027 (2012) 104.
39. N. Shahabadi, S. M. Fili, F. Kheiridoosh, *J. Photochem. Photobiol., B.* 128 (2013) 20.
40. N. Raman, S. Sobha, L. Mitu, *Monatsh Chem.* 143 (2012) 1019.
41. F. Caruso, M. Rossi, A. Benson, C. Opazo, D. Freedman, E. Monti, M.B. Gariboldi, *J. Med. Chem.*55 (2012) 1072.
42. A. Mehdinia, S.H. Kazemi, S.Z. Bathaie, A. Alizadeh, M. Shamsipur, M.F.Mousavi, *Anal. Biochem.* 375 (2008) 331.